

## A Nickel Sublayer: An Improvement in the Electrochemical Performance of Platinum-Based Electrocatalysts as Anodes in Glucose Alkaline Fuel Cells

Behnam Moeini<sup>a,b</sup>, Masoumeh Ghalkhani<sup>a</sup>, Tahereh G. Avval<sup>b</sup>, Matthew R. Linford<sup>b</sup>, Rasol Abdullah Mirzaie<sup>a,\*</sup>

a) Fuel Cell Research Laboratory, Department of Chemistry, Faculty of Science, Shahid Rajaei Teacher Training University, Tehran, Iran

b) Department of Chemistry and Biochemistry, Brigham Young University, C100 BNSN, Provo, Utah 84602, USA

Received 17 November 2020; received in revised form 12 February 2021; accepted 13 February 2021

### ABSTRACT

Platinum–nickel electrocatalysts supported on the modified carbon paper (MCP) were prepared by electrodeposition. Here, various procedures were applied for the electrodeposition of nickel and platinum particles, separately or simultaneously, on the surface of the MCP as an anode electrode for glucose alkaline fuel cells. The establishment of the best procedure for this fabrication is the main goal of this work. The obtained electrocatalysts were characterized by cyclic voltammetry, linear sweep voltammetry, electrochemical impedance spectroscopy (EIS), scanning electron microscopy (SEM), and X-ray photoelectron spectroscopy (XPS). The results showed that the Pt/Ni electrocatalyst, electrodeposited from two separate solutions containing Ni and then Pt ions, has excellent electrocatalytic activity for the glucose oxidation reaction (GOR). On the other hand, the Pt/Ni/MCP electrode showed satisfactory repeatability when subjected to continuous cycling and less concentration polarization in the oxidation region of GOR (from -1 to 0.6 V vs. SCE). Also, the Pt/Ni/MCP electrode showed a significant increase in the exchange current density ( $0.95 \text{ mA cm}^{-2}$ ) that accelerates the kinetics of the glucose oxidation reaction. These results indicate that modification of the catalyst layer structure in the present work is the most promising approach to achieve low-cost and efficient catalysts for use in glucose alkaline fuel cells.

**Keywords:** Platinum–Nickel electrocatalyst; Electrodeposition method; Glucose; Alkaline fuel cell.

### 1. Introduction

With increasing environmental concerns and the increasing need for cheap and renewable energy sources, scientists have focused on clean and safe fuels. These efforts have led to work on new fuel cells that can work with environmentally friendly fuels such as glucose [1]. Regarding the dominant role of the electrode materials in the fuel cell efficiency and to overcome the slow kinetics of the electrode reactions, and electrode poisoning problems, the development of high performance electrocatalysts has received a lot of attention [2-5]. One of the main problems in glucose alkaline fuel cells is the development of an anodic catalyst with high electroactivity towards the glucose oxidation reaction (GOR). Studies on electrocatalytic oxidation of glucose are of high interest to fuel cell res-

earchers because glucose is an abundant, cheap, and non-toxic bio-fuel [6-10]. Unlike hydrogen-based fuel cells, there is no fuel storage problem or explosion danger associated with glucose-based alkaline fuel cells. During the last few decades, many studies on the electro-oxidation of carbohydrates have shown that noble metal catalysts, such as Pt, in alkaline media, improve the rate of GOR [11-19].

Platinum has been extensively employed for modified electrode construction with good electrocatalytic activity toward GOR [20-23]. Pt nanostructures including various shapes, sizes, and morphologies have been chemically or electrochemically synthesized and used as an electrocatalyst for GOR [16]. Reported results revealed that Pt alone [24], or in combination with another metal [25-28], metal oxide [29], or even organic compounds [30] can play an effective role in the

\*Corresponding author:

E-mail address: ra.mirzaei@sru.ac.ir (R. Addullah Mirzaie);

reduction of GOR overvoltage and improvement of analytical sensitivity and performance.

Fast and reversible electron transfer processes have been confirmed for many transition metal oxides such as copper [2, 31, 32] and nickel [33] oxides. The application of transition metals in the preparation of modified electrodes has led to the overpotential reduction of a wide range of reactions [32, 34-37]. Compared to the precious metals [38], non-precious metal oxides exhibited electrocatalytic activity toward carbohydrate oxidation with lack of surface poisoning.

Previously, the electrocatalytic and enhancement effects of Ni electrodes on GOR have been shown [39]. These properties are based on the electron transfer mediation effect of the surface-bound  $\text{Ni}^{2+}/\text{Ni}^{3+}$  redox couple, which is mainly effective in alkaline media [40, 41]. Homogeneous and repeatable deposition with desired nanostructure of the catalyst on the electrode substrate affects the efficiency of the reaction. Metal or metal oxide-based modified electrodes prepared by diverse chemical and electrochemical procedures have been developed for GOR [32, 33, 38]. Electrochemical synthesis has been used as a facile, efficient, and controllable strategy for the deposition of metal and metal oxide nanoparticles on a wide variety of substrates, including glassy carbon [11], carbon paper [42, 43], and carbon nanotubes [44, 45]. This method is affected by many parameters such as solution concentration, applied potential, temperature, and the type of electrolyte [46].

Notably, the synthetic procedure and order of steps in a procedure to make a Pt-based electrocatalyst affect the final catalytic efficiency of the prepared electrode. In this work, we consider the advantages of Pt and Ni in GOR because of the low cost of Ni, where the effect of Ni in the Pt catalyst for GOR was studied. Even though various modified electrodes based on a hybrid nanostructure of Ni and Pt have been developed, a comprehensive comparison of the diverse electrodeposition procedures and optimization of the effective parameters are required to achieve the best fuel cell performance. The development of a fast and facile procedure for preparation of a modified anode electrode applicable for glucose fuel cells with high electrocatalytic activity was the main aim of the present study. Electrocatalyst preparation here was based on electrochemical deposition via cyclic voltammetry. In particular, we have prepared modified carbon paper (MCP) supported Pt-Ni particles by an electrodeposition method in two steps: (I) the MCP substrate was produced and (II) platinum-nickel particles were electrochemically deposited on the surface of an MCP

substrate. In all deposition experiments, the number of successive CV cycles and the potential sweep rate were constant, and the potential range of electrochemical deposition was chosen such that both species (Ni and Pt) could be deposited. Notably, the effect of Ni on the GOR was investigated by two procedures:

- 1) Simultaneous electrodeposition of Pt and Ni on the MCP.
- 2) Layer-by-layer electrodeposition of the Pt and Ni, in which the order of the layers' deposition was also checked.

The activity of the resulting electrocatalysts toward the GOR in 0.3 M glucose and 0.5 M KOH was evaluated by cyclic voltammetry (CV), linear sweep voltammetry (LSV), and electrochemical impedance spectroscopy (EIS).

## 2. Experimental

### 2.1. Materials

In this work we used the following chemicals: Carbon powder (Vulcan XC-72R) Cabot Corporation, carbon paper (Toray 90 T) Japan, Hexachloroplatinic (IV) acid hexahydrate ( $\text{H}_2\text{PtCl}_6 \cdot 6\text{H}_2\text{O}$ ) (~40 % Pt), Orthophosphoric acid ( $\text{H}_3\text{PO}_4$ ) 85 %, 2-propanol (> 99 % pure), D-(+)-glucose; 99.5%, and potassium hydroxide (KOH) (> 85 %, flakes purified) from Merck, Germany. All aqueous solutions were prepared using deionized water.

### 2.2. Electrode preparation

For preparing electrodes, at first, a substrate electrode was made and then used for the electro deposition step. The carbon Vulcan paste was prepared by 30 min sonication of a 2:1:1 mixture solution of water, 2-propanol, and PTFE, respectively adding 3  $\text{mg}/\text{cm}^2$  carbon Vulcan, and heating until reaching a paste. The substrate was fabricated by deposition of 3  $\text{mg}/\text{cm}^2$  of carbon Vulcan paste on the carbon paper sheet with a 1.13  $\text{cm}^2$  geometric area, which was dried by heating at 200 °C for 45 min. The resulting modified carbon paper was named MCP, and it was employed for electrochemical deposition of the electrocatalysts. For electrodeposition, the substrates were immersed in a precursor solution including  $\text{H}_3\text{PO}_4$  (0.5 M),  $\text{H}_2\text{PtCl}_6$  (0.6 mM), and  $\text{NiSO}_4 \cdot 6\text{H}_2\text{O}$  (0.6 M), and then the electrocatalysts were electrodeposited by cyclic voltammetry (CV) technique at 50 mV/s from -0.85 to 0.25 V vs. saturated calomel electrode (SCE) (see **Table 1**). According to the cycling detail in the **Table 1** the electrodes were prepared by electrodeposition of Ni on MCP (Ni/MCP), Pt on MCP (Pt/MCP), Ni on Pt/MCP

(Ni/Pt/MCP), Pt on Ni/MCP (Pt/Ni/MCP), and co-deposition of Ni and Pt on MCP (Pt-Ni/MCP).

### 2.3. Electrochemical Tests

Electrochemical experiments (CV and LSV) were performed in a separator-free three-electrode cell (a cone shape electrochemical cell made from a 75 ml glass container and a PTFE electrode separator, from

Behpajouh Company, Iran). Our prepared electrodes were used as working electrodes, the SCE saturated with KCl was used as the reference electrode, while a platinum sheet was used as the counter electrode. In all experiments, the glucose (fuel) and potassium hydroxide (electrolyte) concentrations were fixed at 0.3M and 0.5 M, respectively.

**Table 1.** Electrodeposition sequence of selected metals

Electrocatalyst	Pt/MCP	Ni/MCP	Ni/Pt/MCP	Pt/Ni/MCP	Pt-Ni/MCP
Deposited metal	Pt	Ni	First Pt and then Ni	First Ni and then Pt	Pt and Ni Simultaneously
Cycle number	30	30	15+15	15+15	30

Electrochemical impedance spectroscopy (EIS) was done within a three-electrode configuration that include the working electrode, a sheet platinum counter electrode and an SCE reference electrode using a potentiostat (IM6ex Zahner. GmbH & Co. KG). Impedance spectra were recorded from 1000 Hz to 10 mHz with an excitation amplitude of 10 mV in KOH solution (0.5 M) and glucose 0.3M at OCV potential. Z view software (v3.4b by Scribner Associates Inc., Southern Pines, NC, and USA) was used for the analysis of EIS data.

### 2.4. Instrumental characterization

Scanning electron microscopy (SEM) was performed with a Helios Nanolab TM 600 instrument (FEI, Hillsboro, OR). XPS was performed with a Surface Science SSX-100 instrument (maintained by Service Physics, Bend, OR, USA) with monochromatic Al K $\alpha$  X-rays, a hemispherical analyzer, and a take-off angle of 35°. Survey scans were obtained in 6 passes with an X-ray spot size of 800 x 800  $\mu\text{m}^2$  and a nominal pass energy of 150 eV (resolution setting of '4' on the instrument). High-resolution scans were collected over the Pt 4f regions centered at a BE of 75 eV with an energy window of 20 eV and a step size of 0.0625 eV. The number of scans was 15, and the spot size was 800 x 800  $\mu\text{m}^2$  with the same nominal pass energy and resolution as the survey scans. Charge compensation was not employed during this data acquisition. Area ratios were calculated, and peak fitting performed, using the CasaXPS modeling software (Casa Software Ltd., Version 2.3.18PR1.0), where the quality of the fits was determined based on the standard deviation of the residuals (STDRes) of a given fit.

A Shirley background was employed for baseline correction [47]. The Pt 4f metallic and oxide spectra were fitted using LA (asymmetric Lorentzian) and

Gaussian-Lorentzian product functions, respectively [48]. All three Pt 4f envelopes were fit using three spin-orbit pairs corresponding to metallic, Pt(II), and Pt(IV). The spin-orbit splitting was constrained to be 3.34 eV for each pair. In all the spectra, the Pt(II) 4f<sub>7/2</sub> and Pt(IV) 4f<sub>7/2</sub> fit components were spaced +1.4, and +3.9 eV, respectively, from the metallic Pt 4f<sub>7/2</sub> component, which was positioned at 71.14 eV [49].

## 3. Result and Discussion

### 3.1. Electrode cyclic deposition diagrams through an acidic platinum and nickel solution

In the present work, the timing and order of the electrodeposition of platinum and nickel particles on the surface of the MCP substrate for their sensitivity toward GOR were investigated. Here, three procedures were employed for the preparation of the GOR electrocatalysts as one element (Ni/MCP or Pt/MCP), layer-by-layer two elements from separate solutions (Pt/Ni/MCP or Ni/Pt/MCP), and co-deposited Ni and Pt particles (Pt-Ni/MCP), by applying overall 30 CV cycles of the appropriate metals' ion solutions. Initially, the voltammetry response of the prepared electrodes was evaluated during electrodeposition of the metal particles on the surface of the MCP electrode, which was the substrate. **Fig. 1** shows the 1<sup>st</sup> and 15<sup>th</sup> CVs recorded during the electrodeposition steps. In the first procedure, Pt particles were deposited directly on the MCP (**Fig. 1A** (a, b)), or on the Ni-modified MCP surface (Ni/MCP) (**Fig. 1A** (c, d)). The current of the 15<sup>th</sup> CV of the Pt deposition on MCP (**Fig. 1A** (b)), was lower than the first scan (**Fig. 1A** (a)), which may be due to a reduction of active sites on the electrode surface after each scan. Notably, the variation of the current responses of Pt deposited on Ni/MCP followed the same behavior as in the case of the bare MCP. Observation of a high current in the negative potential sweep direction

could be related to a facile hydrogen evolution process on the Pt-modified MCP or Ni/MCP.

**Fig. 1B** shows the 1<sup>st</sup> and 15<sup>th</sup> scans of the CVs recorded during Ni electrodeposition on MCP (**Fig. 1B** (a, b)), or on Pt/MCP (**Fig. 1B** (c, d)). Notably, both CVs (**Fig. 1B** (a, b)) show similar behavior with a low current response, which revealed that Ni-modified MCP is not a good electrocatalyst for hydrogen evolution. The CV

response in **Fig. 1B** (c, d) is similar to Pt/MCP or Pt/Ni/MCP, with almost the same current, revealing that Ni deposition on Pt/MCP did not significantly change its response. Simultaneous deposition of Pt and Ni on the MCP surface (Pt-Ni/MCP), (**Fig. 1C**) provided a lower current density than Pt/Ni/MCP or Pt/MCP for the hydrogen evolution reaction which might be due to the occupation of some active surface sites by Ni particles.

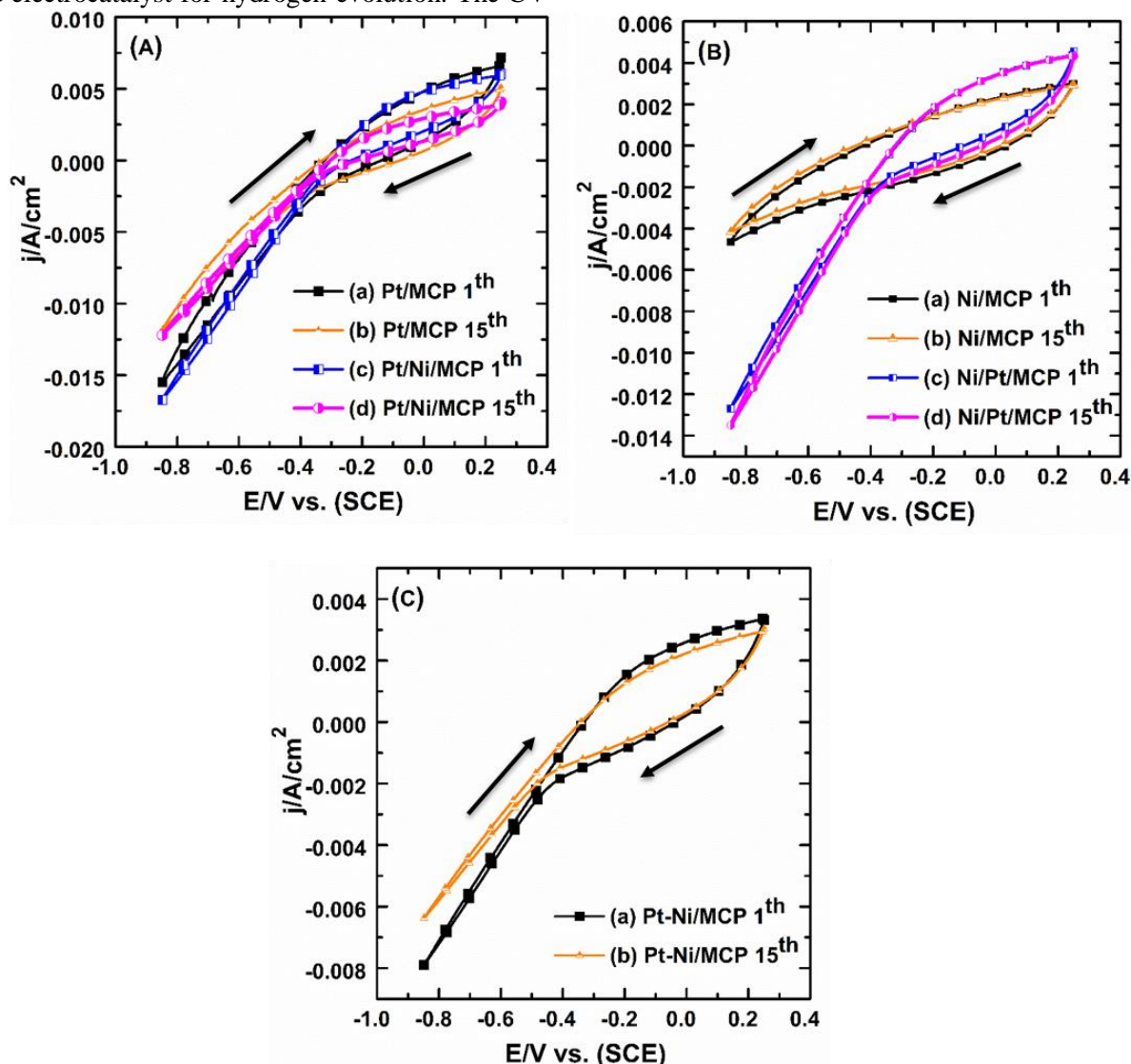


**Fig. 1.** The first (a, c) and 15<sup>th</sup> (b, d) electrodeposition CVs of A) Pt on the MCP (a and b) or Ni/MCP (c and d) surface, B) Ni on the MCP (a and b) or Pt/MCP (c and d) surface and C) Pt-Ni on the MCP (a and b) from -0.85 to 0.25 V vs. SCE at a scan rate of 50 mV/s in 25 °C in a solution of A)  $H_3PO_4$  (0.5 M),  $H_2PtCl_6$  (0.6 mM), B)  $H_3PO_4$  (0.5 M) and  $NiSO_4 \cdot 6H_2O$  (0.6 M), and C)  $H_3PO_4$  (0.5 M),  $H_2PtCl_6$  (0.6 mM), and  $NiSO_4 \cdot 6H_2O$  (0.6 M).

### 3.2. Electrochemical evaluation with respect to GOR

#### 3.2.1 Cyclic voltammetry (CV)

Typical glucose electro-oxidation voltammograms in the literature [1,3,14] depict three oxidation regions at -0.8, -0.3 and 0.3 V vs. SCE in CV. These regions appear in the positive sweep direction due to chemisorption and

dehydrogenation of glucose in the hydrogen wave region, glucose oxidation catalyzed by adsorbed-OH on the catalyst surface in the double-layer region, and surface oxidation of the electrocatalyst, respectively. According to the literature, FTIR and HPLC data obtained from the electrochemical oxidation of d-glucose on the platinum electrode in alkaline medium

show that gluconic acid is a major intermediate of GOR, which may be produced due to the oxidation of the adsorbed intermediate of hydrolysis of glucose- $\gamma$ -lactone [50]. Here, the potential of  $-0.3$  V vs. SCE was chosen as the oxidation potential of glucose in alkaline media at a platinum electrocatalyst [1,8].

**Figs. 2A, B and C** depict CVs of the modified MCPs in  $0.3$  M glucose in  $0.5$  M KOH at three scan rates of  $25$ ,  $50$ , and  $100$  mV/s, respectively. The obtained results reveal that step-by-step electrodeposition of the Pt and Ni on the MCP is more effective than their co-deposition. Also, the best response and catalytic effect were observed when Pt was deposited onto Ni/MCP, **Fig. 2A, B and C** (d). This observation shows that Pt deposition is more favorable on the substrate containing Ni than on the MCP substrate alone. In other words,

modified electrodes having Ni at the outermost surface layer showed no catalytic effect toward GOR under the mentioned working conditions. Here, the most negative OCV resulted in Pt/Ni/MCP, while the most positive OCV was observed for Ni/Pt/MCP. Moreover, CVs recorded at all scan rates for Pt/Ni/MCP showed only an oxidation peak for GOR, which confirmed the irreversibility of the GOR. The electrocatalytic process was studied by plotting the graph of the scan rate-normalized current against the scan rate (**Fig. 2D**). According to these data, a CE (chemical/electrochemical catalytic) mechanism can be suggested for the electro-catalytic oxidation of the glucose at a Pt/Ni/MCP electrode [51, 52]. The comparison of the related current and potential data is shown in **Table 2**.

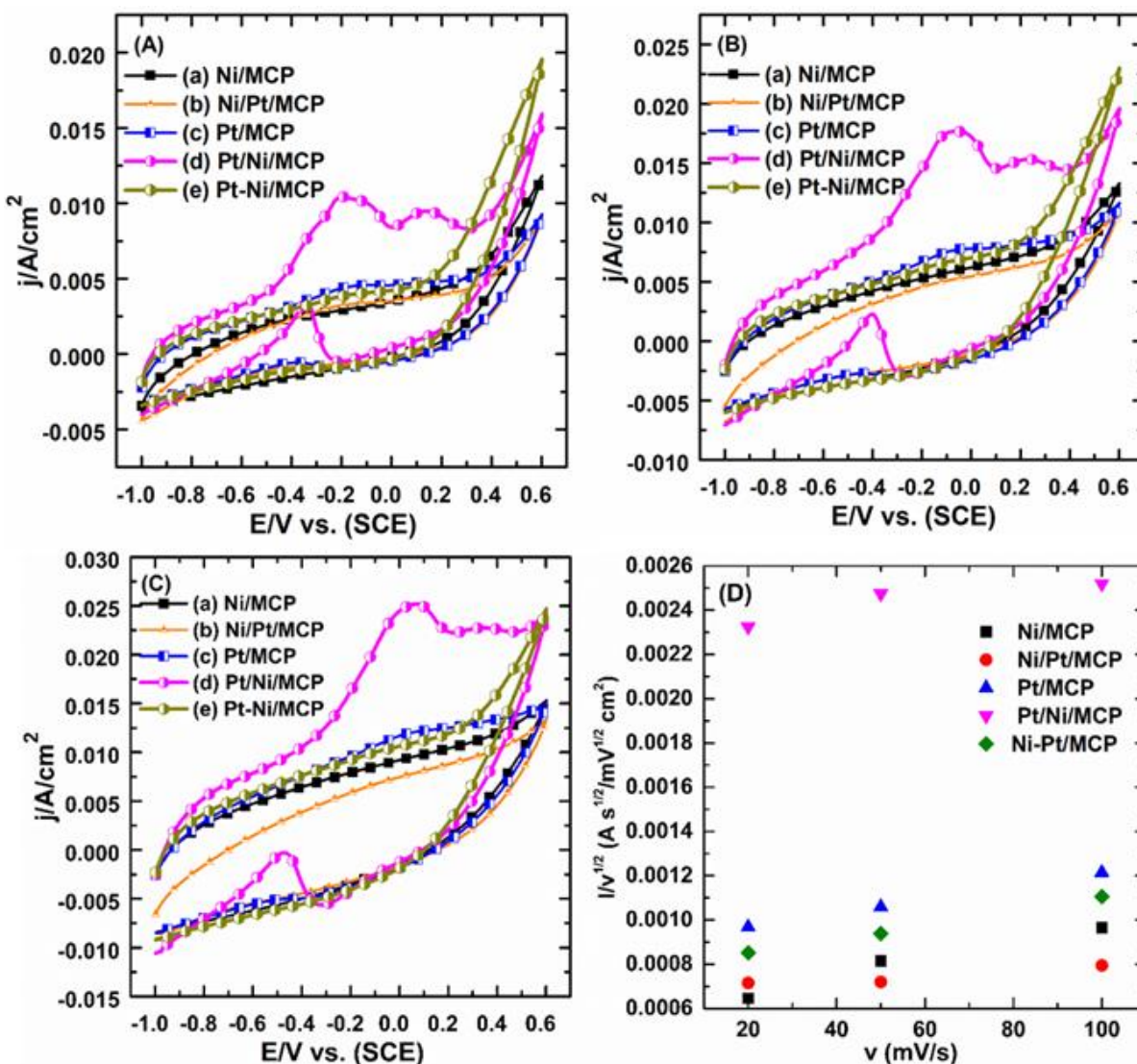


**Fig. 2.** CVs of (a) Ni/MCP, (b) Ni/Pt/MCP, (c) Pt/MCP, (d) Pt/Ni/MCP, and (e) Pt-Ni/MCP electrocatalysts at a scan rate of A)  $20$  mV/s B)  $50$  mV/s and C)  $100$  mV/s in the presence of  $0.3$  M glucose and  $0.5$  M KOH at  $25$  °C, and D) variation of normalized peak currents with scan rate vs. potential scan rate.

**Table 2.** Comparison of the maximum current and starting cathodic current potential for 1<sup>st</sup> and 15<sup>th</sup> CV scans

Electrocatalyst		Pt/MCP	Ni/MCP	Ni/Pt/MCP	Pt/Ni/MCP	Pt-Ni/MCP
<sup>a</sup> $I_{\max}$ (mA/cm <sup>2</sup> ) at -0.85 V	1 <sup>st</sup> CV	-15.57	-4.80	-12.75	-16.80	-7.94
	15 <sup>th</sup> CV	-11.95	-4.19	-13.56	-12.24	-6.40
<sup>b</sup> $E_s$ (V)	1 <sup>st</sup> CV	-0.25	-0.13	-0.27	-0.32	-0.23
	15 <sup>th</sup> CV	-0.22	-0.17	-0.21	-0.34	-0.28
	CV					

a) Maximum cathodic current density. b) Starting cathodic current potential

### 3.2.2 Linear Sweep Voltammetry (LSV)

In agreement with CV, the linear sweep voltammograms in **Fig. 3** show a positive shift of the OCV in the presence of Ni particles at the Ni/Pt/MCP and Ni/MCP electrocatalysts. Obviously, the Pt electrocatalyst deposited on the MCP substrate, which was previously modified by Ni particles, plays a more effective role on the GOR than when Pt was deposited directly on the MCP surface. Also, the Pt particles deposited on the Ni/MCP were a more effective catalyst for GOR than Pt particles that were simultaneously deposited with Ni particles on the MCP. Notably, the better performance of Pt/Ni/MCP led to a higher current and a more negative OCV for GOR. From LSV data, and using the Tafel equation [53], the exchange current density at the rate determining step was calculated, which is a measure of the kinetics of the glucose oxidation reaction on the prepared electrodes. The obtained exchange current densities at Ni/MCP, Ni/Pt/MCP, Pt/MCP, Pt/Ni/MCP and Pt-Ni/MCP electrocatalysts were 0.25, 0.24, 0.39, 0.95 and 0.24 mA cm<sup>-2</sup>, respectively. Evaluation of the exchange current density shows that the presence of nickel in the reaction layer on the platinum substrate or next to the platinum particles of the prepared electrodes does not provide an effective kinetic condition for the glucose oxidation reaction, whereas when the platinum particles are placed on the nickel substrate, compared to the case of pure platinum, the exchange current density has significantly increased. These observations again confirm the importance of the order of the layer-by-layer electrodeposition of the metal catalysts on the MCP surface for GOR.

### 3.2.3 Evaluation of the stability of the constructed electrodes

To estimate the durability of the prepared electrocatalyst, 200 successive CVs were recorded from -1 to 0.6 V vs. SCE. **Fig. 4** shows the 200<sup>th</sup> of these cycles. Variation of the OCV and the current density of

the tested electrodes is listed in **Table 3**. The results illustrate that after 200 cycles, the lowest anodic current density drop occurs for the Pt/Ni/MCP electrocatalyst, which confirms its better performance and stability compared to other Pt-based modified electrodes. Notably, the presence of Ni particles as a sublayer for the Pt electrodeposition provides a suitable substrate with high electronic interaction with Pt particles that creates a strong connection between Pt particles and the electrode surface. This positive effect was evident in the stability tests.

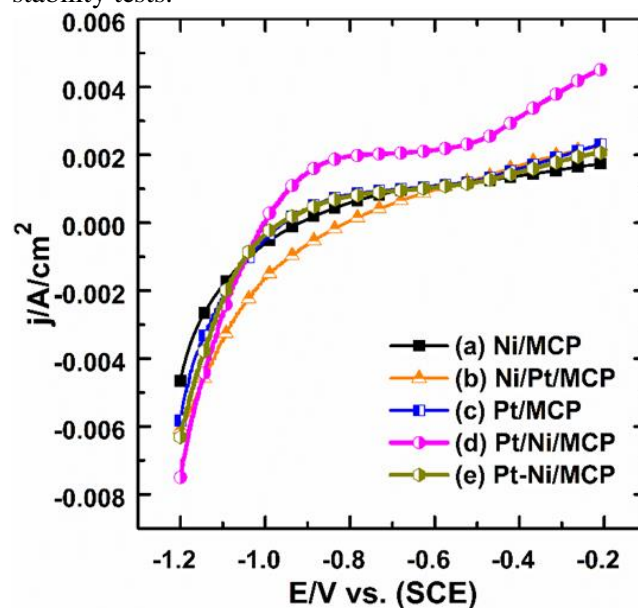


**Fig. 3.** LSVs of (a) Ni/MCP, (b) Ni/Pt/MCP, (c) Pt/MCP, (d) Pt/Ni/MCP, (e) Pt-Ni/MCP electrocatalysts from -1.2 to -0.2 V vs. SCE at a scan rate of 1 mV/s in the presence of 0.3 M glucose and 0.5 M KOH at 25 °C

### 3.2.4 EIS characterization

EIS was also used to evaluate the electro-catalyst performance by means of Nyquist diagrams. Here, impedance spectra were recorded from 1000000 to 0.1 Hz with an excitation amplitude of 10 mV in 0.5 M

KOH containing 0.3 M glucose at -0.3 volt. Fig. 5 shows the resulting Nyquist diagrams of the prepared electrocatalysts. Obviously, the natural resistance of the Pt/MCP (c), Ni/MCP (a), and Ni/Pt/MCP (b) electrocatalysts are close together and greater than the natural resistance of the Pt/Ni/MCP (d) and Pt-Ni/MCP (e) electrocatalysts. The Nyquist diagrams show that the dominant phenomena at the electrode surface are the adsorption of intermediates on the surface of the electrodes. The other effect is the diffusion of the electroactive molecules to the surface of the electrode. The gradient of the Warburg plot was used for the calculation of the Warburg coefficient,  $\sigma$ , as shown in Fig. 6. The diffusion coefficient ( $D$ ) of glucose at the interface of the electrode and the solution was obtained according to Eq. (1) [54].

$$D = R^2 T^2 / 2 A^2 n^4 F^4 C^2 \sigma^2 \quad (1)$$

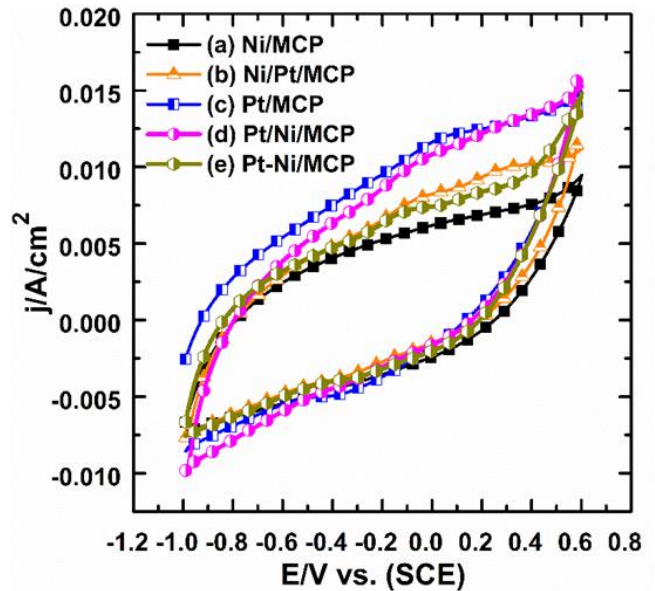


Fig. 4. 200<sup>th</sup> CVs of (a) Ni/MCP, (b) Ni/Pt/MCP, (c) Pt/MCP, (d) Pt/Ni/MCP, and (e) Pt-Ni/MCP electrocatalysts recorded successively from -1.0 to 0.6 V vs. SCE at a scan rate of 100 mV/s in the presence of 0.3 M glucose in 0.5 M KOH at 25 °C

Table 3. Open circuit potential and current data before and after applying 200 cycles.

Electrocatalyst	Pt/MCP	Ni/MCP	Ni/Pt/MCP	Pt/Ni/MCP	Pt-Ni/MCP
OCV	-0.96	-0.92	-0.70	-0.92	-0.95
OCV after 200 cycle	-0.79	-0.78	-0.79	-0.92	-0.83
Current density (mA/cm <sup>2</sup> ) at -0.3 V at the 1 <sup>st</sup> cycle	7.40	7.23	8.64	12.67	8.43
Current density(mA/cm <sup>2</sup> ) at -0.3 V after 200 cycle	4.91	4.68	5.63	8.55	5.40

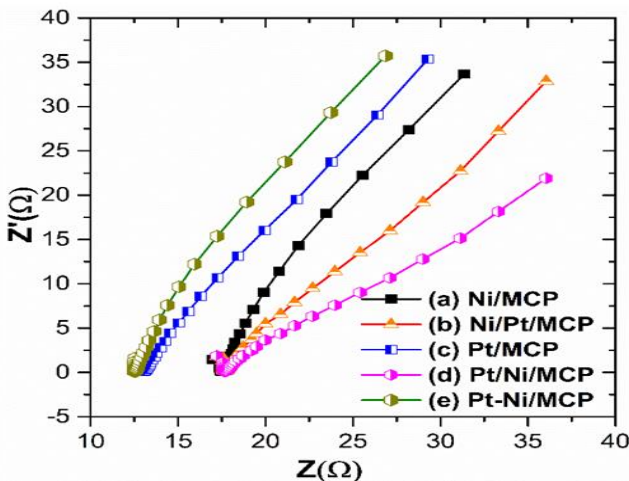


Fig. 5. Nyquist diagrams of (a) Ni/MCP, (b) Ni/Pt/MCP, (c) Pt/MCP, (d) Pt/Ni/MCP, and (e) Pt-Ni/MCP were recorded from 1000 Hz to 10 mHz with an excitation amplitude of 10 mV in KOH solution (0.5 M) and glucose 0.3 M at OCV potential

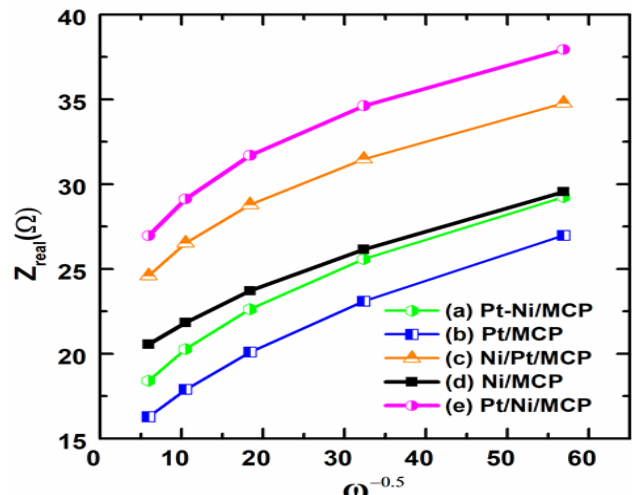


Fig. 6. Warburg plots of (a) Ni/MCP, (b) Ni/Pt/MCP, (c) Pt/MCP, (d) Pt/Ni/MCP, and (e) Pt-Ni/MCP electrocatalysts obtained from the Nyquist diagrams in Fig. 5

where  $D$  is the diffusion coefficient ( $\text{cm}^2 \text{s}^{-1}$ ),  $R$  is the gas constant ( $8.314 \text{ J mol}^{-1} \text{ K}^{-1}$ ),  $T$  is the absolute temperature ( $298.15 \text{ K}$ ),  $A$  is the area of the electrode ( $\text{cm}^2$ ),  $n$  is the number of electrons involved in the redox process,  $C$  is the molar concentration of reactants in the tested electrode,  $F$  is the Faraday constant, and  $\sigma$  is the Warburg impedance coefficient. The obtained results in **Table 4** reveal the lowest  $D'$  ( $n4D$ ) for the Pt/MCP electrode ( $2.71 \times 10^{-11} \text{ cm}^2 \text{ s}^{-1}$ ) and the highest  $D'$  ( $3.86 \times 10^{-11} \text{ cm}^2 \text{ s}^{-1}$ ) for Ni/MCP electrode, albeit the variation

range of the obtained  $D'$  values for various examined electrodes was limited. Notably, the presence of Ni in the reaction layer of the prepared electrodes led to an enhancement of the diffusion coefficient of glucose toward the electrified interface, which can be beneficial for the Pt electrocatalyst in the Pt/Ni/MCP electrode. In other words, in an optimized electrocatalyst, favorable conditions for the glucose oxidation reaction occur in a diffusion controlled manner with fast kinetics process, which leads to the excellent performance with GOR.

**Table 4.** Diffusion coefficient of the electrodes

Electrocatalyst	Pt/MCP	Ni/MCP	Ni/Pt/MCP	Pt/Ni/MCP	Pt-Ni/MCP
Diffusion coefficient ( $n4D$ ) ( $\text{cm}^2/\text{s}$ )	2.71 E-11	3.86 E-11	2.74 E -11	3.14 E-11	2.73 E-11

### 3.3. SEM and XPS analysis

The SEM images of the optimized electrode, Pt/Ni/MCP (**Fig. 7a**) showed highly dispersed spherical platinum particles. The SEM images also confirmed that nickel is significantly covered with platinum. **Fig. 7b** and **c**

showed a few needle-like platinum particles in addition to the common spherical Pt particles. Although we could not distinguish Ni from Pt atoms by SEM, EDX of the Pt/Ni/MCP electrode in **Fig. 7d** confirmed the presence of Ni at the electrode's surface.

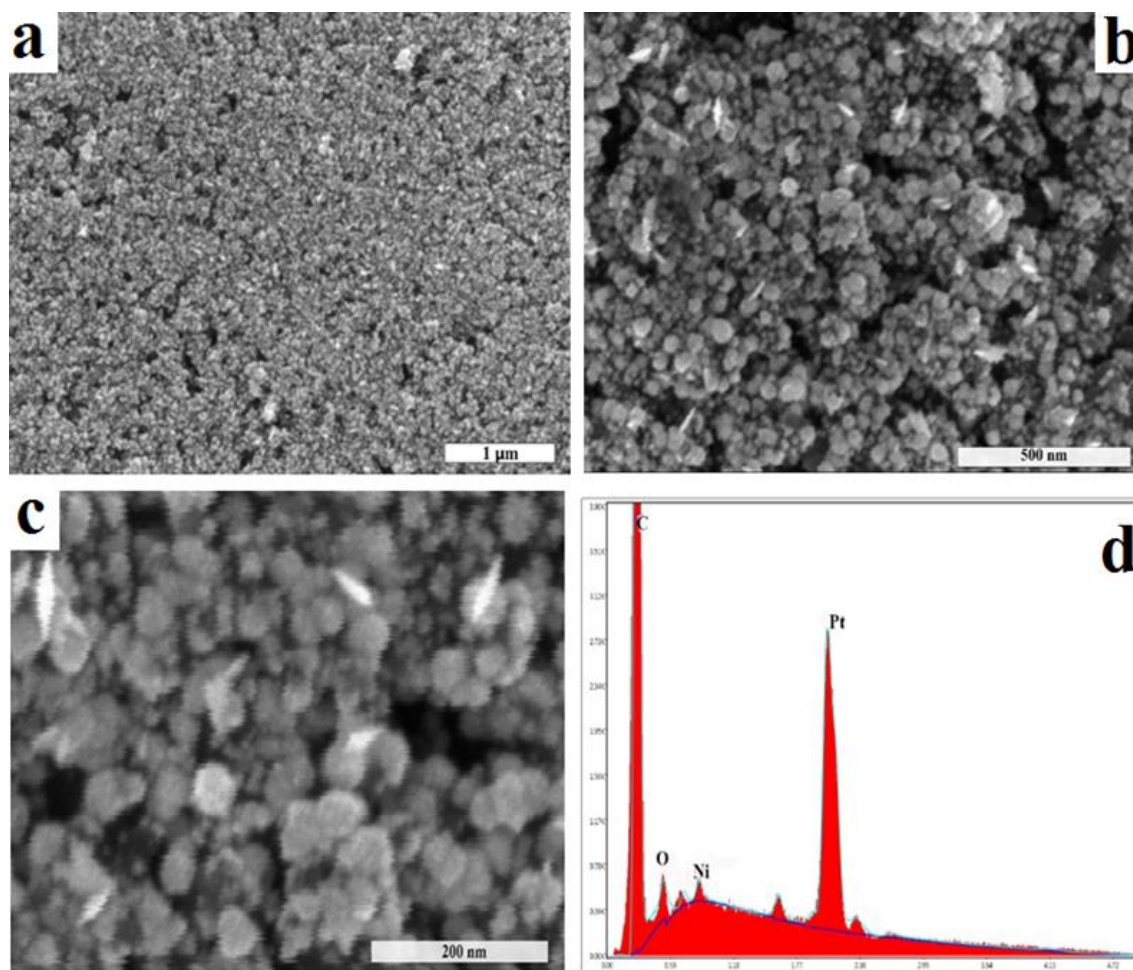


**Fig. 7.** (a, b and c) SEM images of the Pt/Ni/MCP electrode with various magnification and (d) EDX

The XPS survey spectra of Pt/Ni/MCP in **Fig. 8a** confirmed the presence of Pt and Ni at the electrode's surface. The high Pt/Ni signal ratio suggests that platinum atoms cover most of the nickel atoms. The Pt 4f regions were employed to obtain additional information about the oxidation states of platinum (**Fig. 8b**). This electrode exhibited three spin-orbit doublets ( $4f_{7/2}$  and  $4f_{5/2}$ ) in different oxidation states. The lower binding energy pair of peaks around 71.3 and 74.6 eV are attributed to Pt in its metallic state. The Pt  $4f_{7/2}$  Pt(II) and Pt(IV) peaks are seen around 72.7 and 75.2 eV, respectively. The quantitative analysis (area ratios) of these Pt species revealed that the prevalence of the platinum atom oxidation states is Pt(0) > Pt(II) > Pt(IV). According to the electrochemical and XPS results, it can be stated that the coating of nickel particles by platinum particles, which are mainly in the form of atomic platinum particles, affects the electronic structure of the optimized electro-catalyst so that this change leads to significant acceleration of the glucose oxidation reaction kinetics with respect to platinum and nickel pure states.

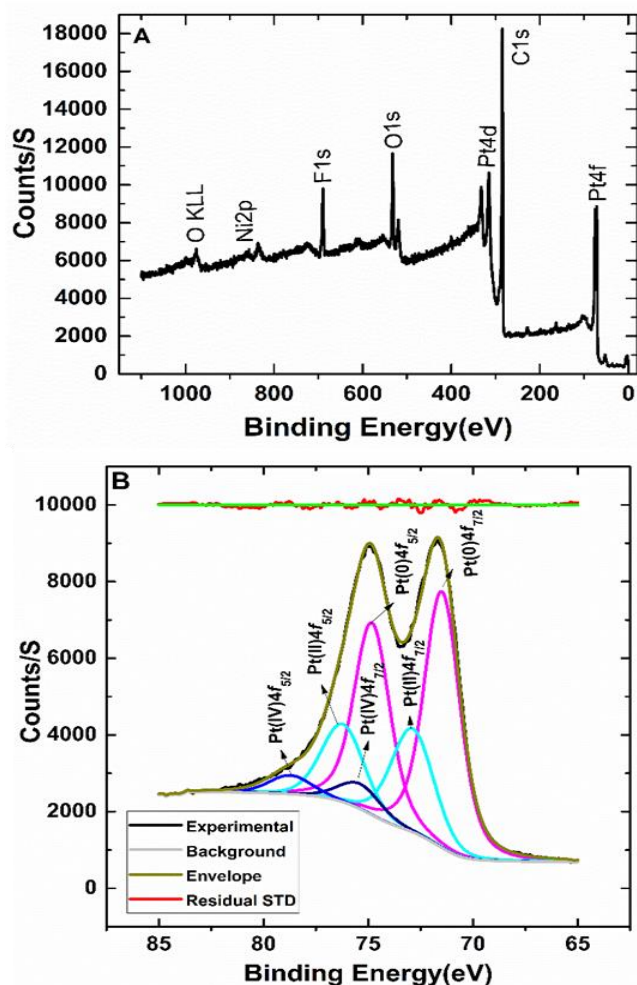


**Fig. 8.** A) XPS survey spectra and B) Pt 4f XPS signals of the Pt/Ni/MCP electrode

## 4. Conclusions

A platinum–nickel electrocatalyst with a layer-by-layer electrodeposited structure (Pt/Ni/MCP) was synthesized from solutions of the corresponding metals. The catalytic activity of the synthesized catalyst for GOR was affected by the layered structure of the catalyst. When the first layer is Ni, which is then covered by Pt, the best catalytic activity is achieved. It seems that the electronic properties of platinum are affected by the nickel substrate and provide favorable conditions for the kinetics of the glucose oxidation reaction. The effect of an uncoated nickel substrate on glucose diffusion to the electrode surface should also be noted. The prepared catalyst exhibits satisfactory reproducibility and good open circuit potential as an anode for glucose alkaline fuel cells. In spite of the reduction of the electrodeposition time of the Pt, the presence of Ni as a sublayer on the MCP in the Pt electrodeposition step led to an improvement of the electrode efficiency for GOR compared to only Pt on the MCP. This is not only related to the presence of Ni because the simultaneous deposition of Ni and Pt did not show the same effect of Ni as a sublayer of Pt. Therefore, it can be noted that the synergy between platinum and nickel provides optimal conditions for the glucose oxidation reaction. Finally, the present study is important because of the decrease in price associated with replacing some of the Pt particles in the electrocatalyst with Ni particles.

## Acknowledgements

The authors would like to acknowledge the support of the Fuel Cell Research laboratory of Shahid Rajaei Teacher Training University (Tehran, Iran).

## References

- [1] D. Basu, S. Basu, A study on direct glucose and fructose alkaline fuel cell. *Electrochim. Acta* 55 (20) (2010) 5775–5779.
- [2] G. Zang, W. Hao, X. Li, S. Huang, J. Gan, Z. Luo, Y. Zhang, Copper nanowires-MOFs-graphene oxide hybrid nanocomposite targeting glucose electro-oxidation in neutral medium. *Electrochim. Acta* 277 (2018) 176-184.
- [3] A. Ehsani, M. Hadi, E. Kowsari, S. Doostikhah, J. Torabian, Electrocatalytic oxidation of ethanol on the surface of the POAP/ phosphoric acid-doped ionic liquid-functionalized graphene oxide nanocomposite film. *Iranian J. Catal.* 7(3) (2017) 187-192.
- [4] M. H. Nobahari, A. Nozad Golikand, M. Bagherzadeh, Synthesis and characterization of Pt<sub>3</sub>Co bimetallic nanoparticles supported on MWCNT as an electrocatalyst for methanol oxidation, *Iranian J. Catal.* 7(4) (2017) 327-335.
- [5] S. Sohrabi, M. Ghalkhani, Metal–organic frameworks as electro-catalysts for oxygen reduction reaction in

- electrochemical technologies, *J. Electronic Mater.* 48 (2019) 4127-4137.
- [6] J. O. Bockris, B. J. Piersma; Gileadi, E. Anodic oxidation of cellulose and lower carbohydrates. *Electrochim. Acta* 9 (10) (1964) 1329-1332.
- [7] J. Chen, C. X. Zhao, M. M. Zhi, K. Wang, L. Deng, G. Xu, Alkaline direct oxidation glucose fuel cell system using silver/nickel foams as electrodes. *Electrochim. Acta*, 66 (2012) 133-138.
- [8] I. V. Delidovich, B. L. Moroz, O. P. Taran, N. V. Gromov, P. A. Pyrjaev, I. P. Prosvirin, V. I. Bukhtiyarov, V. N. Parmon, Aerobic selective oxidation of glucose to gluconate catalyzed by Au/Al<sub>2</sub>O<sub>3</sub> and Au/C: impact of the mass-transfer processes on the overall kinetics. *Chem. Eng. J.* 223 (2013) 921-931.
- [9] El-Refaei, S. M.; Saleh, M. M.; Awad, M. I. Enhanced glucose electrooxidation at a binary catalyst of manganese and nickel oxides modified glassy carbon electrode. *J. Power Sources* 223 (2013) 125-128.
- [10] A. Habrioux, K. Servat, T. Girardeau, P. Guérin, T. W. Napporn, K. B. Kokoh, Activity of sputtered gold particles layers towards glucose electrochemical oxidation in alkaline medium. *Curr. Appl. Phys.* 11 (5) (2011) 1149-1152.
- [11] N. Arjona, M. Guerra-Balcazar, G. Trejo, J. Ledesma-Garcia, L. G. Arriaga, Electrochemical growth of au architectures on glassy carbon and their evaluation toward glucose oxidation reaction. *New J. Chem.*, 36 (12) (2012) 2555-2561.
- [12] D. Basu, S. Basu, Synthesis and characterization of Pt–Au/C catalyst for glucose electro-oxidation for the application in direct glucose fuel cell. *Int. J. Hydrogen Energy*, 36 (22) (2011) 14923-14929.
- [13] D. Basu, S. Sood, S. Basu, Performance comparison of Pt–Au/C and Pt–Bi/C anode catalysts in batch and continuous direct glucose alkaline fuel cell. *Chem. Eng. J.* 228 (2013) 867-870.
- [14] C. Jin, Z. Chen, Electrocatalytic oxidation of glucose on gold–platinum nanocomposite electrodes and platinum-modified gold electrodes. *Synth. Met.* 157 (13-15) (2007) 592-596.
- [15] S. Kerzenmacher, U. Kräling, M. Schroeder, R. Brämer, R. Zengerle, F. von Stetten, Raney-platinum film electrodes for potentially implantable glucose fuel cells. Part 2: glucose-tolerant oxygen reduction cathodes. *J. Power Sources*, 195 (19) (2016) 6524-6531.
- [16] A. Kloke, C. Kohler, R. Gerwig, R. Zengerle, S. Kerzenmacher, Cyclic electrodeposition of ptcu alloy: facile fabrication of highly porous platinum electrodes. *Adv. Mater.* 24 (21) (2012) 2916-2921.
- [17] X. Yan, X. Ge, S. Cui, Pt-decorated nanoporous gold for glucose electrooxidation in neutral and alkaline solutions. *Nanoscale Res. Lett.* 6 (1) (2011) 1-6.
- [18] H. Zhang, N. Toshima, Glucose oxidation using au-containing bimetallic and trimetallic nanoparticles. *Catal. Sci. Technol.* 3 (2) (2013) 268-278.
- [19] R. A. Mirzaie, B. Moeini, Study of type of electrolyte effect on platinum electro-catalyst performance prepared by cyclic voltammetry electrodeposition method for glucose oxidation reaction. *MATTER Int. J. Sci. Technol.* 1 (2015) 91-102.
- [20] I. Taurino, G. Sanzó, F. Mazzei, G. Favero, G. De Micheli, S. Carrara, Fast synthesis of platinum nanopetals and nanospheres for highly-sensitive non-enzymatic detection of glucose and selective sensing of ions. *Sci. Rep.* 5 (1) (2015) 15277.
- [21] D. W. Hwang, S. Lee, M. Seo, T. D. Chung, Recent advances in electrochemical non-enzymatic glucose sensors – A Review. *Anal. Chim. Acta*, 1033 (2018) 1-34.
- [22] T. Unmüssig, A. Weltin, S. Urban, P. Daubinger, G. A. Urban, J. Kieninger, Non-Enzymatic Glucose Sensing Based on Hierarchical Platinum Micro-/Nanostructures. *J. Electroanal. Chem.* 816 (2018) 215-222.
- [23] M. Frei, J. Martin, S. Kindler, G. Cristiano, R. Zengerle, S. Kerzenmacher, Power supply for electronic contact lenses: abiotic glucose fuel cells vs. Mg/Air batteries. *J. Power Sources*, 401 (2018) 403-414.
- [24] X. Tian, S. Lian, L. Zhao, X. Chen, Z. Huang, X. Chen, A novel electrochemiluminescence glucose biosensor based on platinum nanoflowers/graphene oxide/glucose oxidase modified glassy carbon electrode. *J. Solid State Electrochem.* 18 (9), (2014) 2375-2382.
- [25] M. Frei, C. Köhler, L. Dietel, J. Martin, F. Wiedenmann, R. Zengerle, S. Kerzenmacher, Pulsed electrodeposition of highly porous pt alloys for use in methanol, formic acid, and glucose fuel cells. *ChemElectroChem*, 5 (7) (2018) 1013-1023.
- [26] K. Abdul Razak, S. H. Neoh, N. S. Ridhuan, N. Mohamad Nor, Effect of platinum-nanodendrite modification on the glucose-sensing properties of a zinc-oxide-nanorod electrode. *Appl. Surf. Sci.*, 380 (2016) 32-39.
- [27] N. Neha, B. S. R. Kouamé, T. Rafaideen, S. Baranton, C. Coutanceau, Remarkably efficient carbon-supported nanostructured platinum-bismuth catalysts for the selective electrooxidation of glucose and methyl-glucoside. *Electrocatalysis* 12 (2021) 1-14.
- [28] K. A. Soliman, L. A. Kibler, D. M. Kolb, Electrocatalytic behaviour of epitaxial Ag(111) overlayers electrodeposited onto noble metals: electrooxidation of d-glucose. *Electrocatalysis*, 3 (3) (2012) 170-175.
- [29] Q. Sheng, H. Mei, H. Wu, X. Zhang, S. Wang, PtxNi/C nanostructured composites fabricated by chemical reduction and their application in non-enzymatic glucose sensors. *Sensors Actuators B Chem.*, 203 (2014) 588-595.
- [30] C. Chen, R. Ran, Z. Yang, R. Lv, W. Shen, F. Kang, Z.H. Huang, An efficient flexible electrochemical glucose sensor based on carbon nanotubes/carbonized silk fabrics decorated with pt microspheres. *Sensors Actuators B Chem.*, 256 (2018) 63-70.
- [31] H. Shi, S. Zhou, X. Feng, H. Huang, Y. Guo, W. Song, Titanate nanotube forest/CuxO nanocube hybrid for glucose electro-oxidation and determination. *Sens. Actuators B: Chem.* 190 (2014) 389-397.
- [32] L. Parashuram, S. Sreenivasa, S. Akshatha, V. Udayakumar, Sandeep Kumar, S. A non-enzymatic electrochemical sensor based on ZrO<sub>2</sub>: Cu (I) nanosphere modified carbon paste electrode for electro-catalytic

oxidative detection of glucose in raw Citrus aurantium var. sinensis. Food Chem. 300 (2019) 125178.

[33] Y. Gu, H. Yang, B. Li, J. Mao, Y. An, A ternary nanooxide NiO-TiO<sub>2</sub>-ZrO<sub>2</sub>/SO<sub>4</sub><sup>2-</sup> as efficient solid superacid catalysts for electro-oxidation of glucose. Electrochim. Acta 194 (2016) 367-376.

[34] F. Alidusty, A. Nezamzadeh-Ejhih. Considerable decrease in overvoltage of electrocatalytic oxidation of methanol by modification of carbon paste electrode with Cobalt (II)-clinoptilolite nanoparticles. Inter. J. Hydrogen Energy 41 (2016) 8881-8892.

[35] A. Ahmadi, A. Nezamzadeh-Ejhih, A comprehensive study on electrocatalytic current of urea oxidation by modified carbon paste electrode with Ni (II)-clinoptilolite nanoparticles: Experimental design by response surface methodology. J. Electroanal. Chem. 801 (2017) 328-337.

[36] M. S. Tohidi, A. Nezamzadeh-Ejhih. A simple, cheap and effective methanol electrocatalyst based of Mn (II)-exchanged clinoptilolite nanoparticles. Inter. J. Hydrogen Energy 41 (2016) 6288-6299.

[37] R. A. Mirzaie, F. Hamed, Introducing Pt/ZnO as a new non carbon substrate electro catalyst for oxygen reduction reaction at low temperature acidic fuel cells. Iranian J. Catal. 5(3) (2015) 275-283.

[38] G. A. B. Melloa, W. Cheuquepán, V. Briega-Martos, M. J. Feliu, Glucose electro-oxidation on Pt (100) in phosphate buffer solution (pH 7): A mechanistic study. Electrochim. Acta, 354 (2020) 136765.

[39] M. Fleischmann, K. Korinek, D. Pletcher, The kinetics and mechanism of the oxidation of amines and alcohols at oxide-covered nickel, silver, copper, and cobalt electrodes. J. Chem. Soc. Perkin Trans. 2, (10) (1972) 1396-1403.

[40] G. Yang, E. Liu, N. W. Khun, S. P. Jiang, Direct electrochemical response of glucose at nickel-doped diamond like carbon thin film electrodes. J. Electroanal. Chem. 627 (1-2) (2009) 51-57.

[41] M. A. Al-Omair, A. H. Touny, F. A. Al-Odail, M. M. Saleh, Electrocatalytic oxidation of glucose at nickel phosphate nano/micro particles modified electrode. Electroanalysis 8 (4) (2017) 340-350.

[42] H. Gharibi, R. A. Mirzaie, E. Shams, M. Zhiani, M. Khairmand, preparation of platinum electrocatalysts using carbon supports for oxygen reduction at a gas-diffusion electrode. J. Power Sources, 139 (1-2) (2005) 61-66.

[43] M. Pasta, L. Hu, F. La Mantia, Y. Cui, Electrodeposited gold nanoparticles on carbon nanotube-textile: anode material for glucose alkaline fuel cells. Electrochem. commun. 19 (2012) 81-84.

[44] S. Prilutsky, P. Schechner, E. Bubis, V. Makarov, E. Zussman, Y. Cohen, anodes for glucose fuel cells based on carbonized nanofibers with embedded carbon nanotubes. Electrochim. Acta, 55 (11), (2010) 3694-3702.

[45] M. Shamsipur, M. Najafi, M. R. M. Hosseini, Highly improved electrooxidation of glucose at a nickel (ii) oxide/multi-walled carbon nanotube modified glassy carbon electrode. Bioelectrochemistry, 77 (2) (2010) 120-124.

[46] H. Zhang, F. Jiang, R. Zhou, Y. Du, P. Yang, C. Wang, J. Xu, Effect of deposition potential on the structure and

electrocatalytic behavior of Pt micro/nanoparticles. Int. J. Hydrogen Energy, 36 (23) (2011) 15052-15059.

[47] D. A. Shirley, High-Resolution X-Ray Photoemission Spectrum of the Valence Bands of Gold. Phys. Rev. B 5 (12) (1972) 4709-4714.

[48] V. Jain, M. C. Biesinger, M. R. Linford, The gaussian-lorentzian sum, product, and convolution (Voigt) functions in the context of peak fitting X-Ray photoelectron spectroscopy (XPS) narrow scans. Appl. Surf. Sci. 447 (2018) 548-553.

[49] E. Willinger, A. Tarasov, R. Blume, A. Rinaldi, O. Timpe, C. Massué, M. Scherzer, J. Noack, R. Schlögl, M. G. Willinger, Characterization of the platinum-carbon interface for electrochemical applications. ACS Catal. 7(7) (2017) 4395-4407.

[50] G. Moggia, T. Kenis, N. Daems, T. Breugelmanns, Electrochemical oxidation of d-glucose in alkaline medium: impact of oxidation potential and chemical side reactions on the selectivity to d-gluconic and d-glucaric acid. ChemElectroChem, 7 (1) (2020) 86-95.

[51] M. H. Sheikh-Mohseni, A. Nezamzadeh-Ejhih, Modification of carbon paste electrode with ni-clinoptilolite nanoparticles for electrocatalytic oxidation of methanol. Electrochim. Acta, 147 (2014) 572-581.

[52] T. Tamiji, A. Nezamzadeh-Ejhih, Electrocatalytic determination of Hg (II) by the modified carbon paste electrode with Sn (IV)-clinoptilolite nanoparticles. Electroanalysis 10 (5) (2019) 466-476.

[53] T. Tamiji, A. Nezamzadeh-Ejhih, A comprehensive kinetic study on the electrocatalytic oxidation of propanols in aqueous solution, Solid State Sci. 98 (2019) 106033.

[54] L. J. Z. Wang, X. He, J. Gao, J. Li, C. Wan, Ch. Jing. Electrochemical impedance spectroscopy (EIS) Study of LiNi<sub>1/3</sub>Co<sub>1/3</sub>Mn<sub>1/3</sub>O<sub>2</sub> for Li-Ion Batteries. Int. J. Electrochem. Sci. 7 (1) (2012) 345-353.